International Journal of Mass Spectrometry 277 (2008) 291–295

Contents lists available at ScienceDirect

International Journal of Mass Spectrometry

journal homepage: www.elsevier.com/locate/ijms

Negative ion formation by low energy electron attachment to gas-phase 5-nitrouracil

Sylwia Ptasińska[a,*], Elahe Alizadeh[b], Philipp Sulzer[b], Robert Abouaf[c], Nigel J. Mason[a], Tilmann D. Märk[b], Paul Scheier[b]

[a] Department of Physics and Astronomy, The Open University, Walton Hall, MK7 6AA Milton Keynes, United Kingdom
[b] Institut für Ionenphysik and Angewandte Physik, Universität Innsbruck, Technikerstr. 25, 6020 Innsbruck, Austria
[c] Laboratoire des Collisions Atomiques et Moléculaires (UMR 8625), Bâtiment 351, Université Paris-Sud, 91405 Orsay Cedex, France

ARTICLE INFO

Article history:
Received 30 March 2008
Received in revised form 10 June 2008
Accepted 15 June 2008
Available online 21 June 2008

Keywords:
Electron attachment
Dissociative electron attachment
Radiosensitizers

ABSTRACT

Dissociative electron attachment (DEA) to gas phase 5-nitrouracil (5NU) is studied using a double focusing sector field mass spectrometer and a hemispherical electron monochromator (HEM) combined with a quadrupole mass spectrometer (QMS). Besides the formation of the long-lived parent anion $5NU^-$, low energy electron impact (<20 eV) leads to a number of anionic fragments. The ion yield for all observed negative ions has been recorded as a function of the incident electron energy. The most dominant negative ion observed was $(5NU–NO_2)^-$, which is produced directly in the ion source and also weakly as a product of a metastable decay of $5NU^-$. These experiments were supported by quantum chemical calculations based on the density functional theory to calculate the electrostatic potential and molecular orbitals.

1. Introduction

One of the major challenges of modern medical research is to discover the most effective method and pharmaceuticals for cancer treatment [1,2]. Radiotherapy, combining the use of ionizing radiation and the incorporation of radiosensitizers within the tumor cells, has been developed as an alternative and/or complementary treatment to the traditional surgery and to chemotherapy. Radiotherapy is based on the assumption that applied ionizing radiation causes DNA damage. However, the methodology for targeting cancerous rather than healthy cells remains uncertain. Energy deposition by high-energy quanta creates many secondary electrons with an average initial kinetic energy up to 20 eV [3,4] which can induce direct damage at selective sites in the DNA leading to single or double strand breaks. Recent research suggests that control of such electron-induced processes may provide a method for targeting cancerous cells by incorporating radiation sensitive molecules in the DNA of such cells, indeed the effectiveness of compounds used as 'radiosensitizers' has been shown to be related to their interaction with low energy electrons [5].

Pyrimidines have a special place in the drugs used for radiotherapy. The modified pyrimidine bases, especially substituted uracil derivatives, have been widely used due to their importance as the constituents of nucleic acids and useful biological activity [6]. 5-Substituted uracils exhibit a significant pharmacological activity and have been used as antitumor, antibacterial and antiviral drugs. The most prominent representatives are: 5-fluorouracil [6,7] and 5-bromouracil [8,9]. It has been shown that the substitution of thymine nucleobase in genetic sequence of cellular DNA does not change the normal gene expression in non-irradiated cell [10]; however, it leads to increased sensitivity of living cells to X-rays (by factor of four) [11]. Apart from the halogen-modified nucleobases several aromatic nitro compounds also show promise as radiosensitizers for overcoming the radioprotection afforded some tumor cells by their lack of oxygen, 'hypoxia' [12]. The effectiveness of these compounds as radiosensitizers has been shown to be related to the electron affinity of their nitro group. Moreover, many derivatives of 5-nitrouracil (5NU) have shown the following effects: antibacterial activity [13], antitumor activity on leukemia cells [14] and inhibitory effect on macrophage [15], while there are many publications concerning the synthesis of new 5NU derivatives which can be considered as promising candidates for pharmacological agents [16].

In order to understand the molecular mechanisms by which radiosensitizers operate, the interaction of low energy electrons with many isolated gas phase halogenated nucleobases has been studied [17–25]. However, to date, experiments on the interaction of slow electrons with 5-nitrouracil are limited to our recent work on vibrational and electronic excitations and negative ion formation [26]. However this was a preliminary study being limited to a

* Corresponding author. Tel.: +44 190 885 8243.
E-mail address: s.ptasinska@open.ac.uk (S. Ptasińska).

1387-3806/$ – see front matter © 2008 Elsevier B.V. All rights reserved.
doi:10.1016/j.ijms.2008.06.008

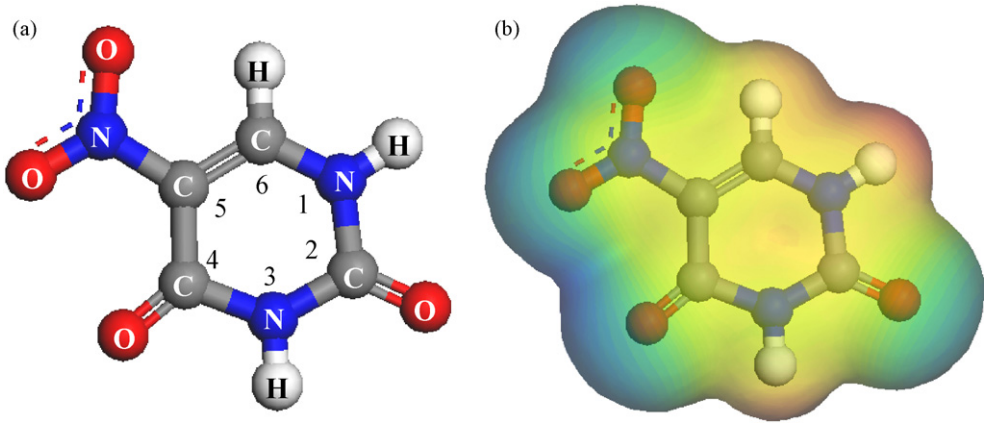

Fig. 1. (a) Molecular structure and (b) the electrostatic potential map of 5-nitrouracil calculated with DMol3 program.

narrow range of electron energy, 0–2 eV and only the three most abundant ions were recorded. In this work we report the results of an extended study on anion production via electron attachment to 5-nitrouracil.

2. Experimental setup

Two apparatus were used in the present studies, a high-resolution double sector field mass spectrometer (VG-ZAB) and a hemispherical electron monochromator (HEM) in combination with a quadrupole mass spectrometer (QMS). Only a brief description of the experimental arrangements is given here, since more details can be found in Ref. [27]. The VG-ZAB apparatus is utilized for measurements requiring high mass resolution, high sensitivity and the HEM instrument for high electron energy resolution.

The neutral target beam is produced by a resistively heated oven containing 5-nitrouracil powder operated at a temperature of 150 °C. The sample was purchased from Sigma–Aldrich with a stated purity of 98% and used without further purification.

In the case of the VG-ZAB apparatus, an effusive beam of 5NU is introduced into a Nier-type ion source where it is crossed with the electron beam. The energy resolution of the electron beam is approximately 0.8 eV at an electron current of 10 μA. The anions formed in the ion source were extracted by a weak electric field and accelerated through a potential drop of 5 kV into the mass spectrometer. The utilized mass spectrometer has a reversed geometry, i.e., magnetic sector field followed by the electric sector field. Additionally, by using this apparatus metastable decay upon dissociative electron attachment (DEA) can be measured. Metastable dissociation in the field-free region between the magnetic and electric sector is studied by mass-analyzed ion kinetic energy scans (MIKE) [28].

The electron beam formed in HEM is set at an energy resolution of about 100 meV and an electron current of 15–25 nA. The effusive beam of 5NU is crossed perpendicularly by the electron beam. Negative ions formed in the collision chamber are extracted by a weak electric field towards the entrance of the QMS. Anion yields were recorded as a function of the electron energy. The electron energy scale is calibrated by means of well-known Cl^- signal from DEA to CCl_4 yielding a narrow peak near zero eV and a weak peak located at 0.8 eV [29]. In both cases, the mass selected negative ions were detected by a channeltron detector.

3. Quantum chemical calculations

To support the experimental work electrostatic potential and molecular orbitals were calculated using the DMol3 software from Accelrys Software Inc. [30]. Quantum chemical calculations based on the use of the density functional theory have been performed. A geometry optimization was performed to determine the minimum-energy structure of a molecule, starting from the initial geometry entered. After the geometry is minimized, other properties are computed. DMol3 supports several non-local exchange and correlation functionals. In the present calculations, the Becke exchange functional (B88) is used in conjunction with the Lee–Yang–Parr correlation functional (BLYP). This so-called generalized gradient corrected (GGA) functional, by Perdew and Wang (P91) was derived by considering low- and high-density regimes and by enforcing various summation rules [30]. The electrostatic potential map and molecular orbitals of 5NU were calculated using the double numerical plus polarization (DNP) basis set, i.e., functions with angular momentum one higher than that of highest occupied orbital in free atom.

4. Results and discussion

4.1. Electron attachment

In contrast to the uracil nucleobase [31], low energy electron impact on 5-nitrouracil (Fig. 1a) induces the formation of the parent negative ion $(5NU)^-$ observed within a very narrow resonance at zero eV, shown in Fig. 2. Additionally, Fig. 2 presents the negative mass spectrum for the region of the parent ion obtained by

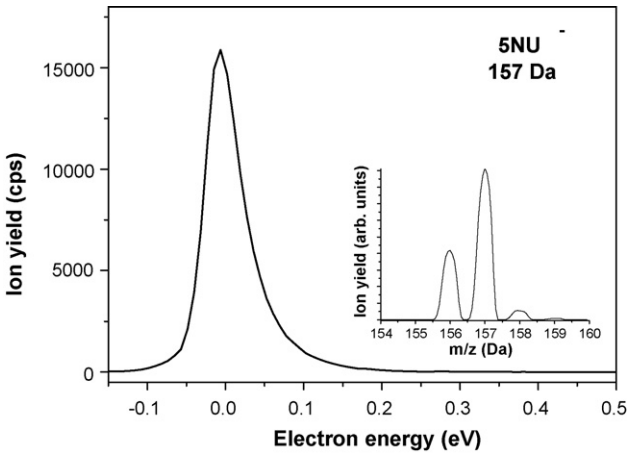

Fig. 2. The anion yield observed for the molecular parent anion $(5NU)^-$. The insert graph shows the anion mass spectrum for the region of the parent anion obtained at 0 eV electron energy.

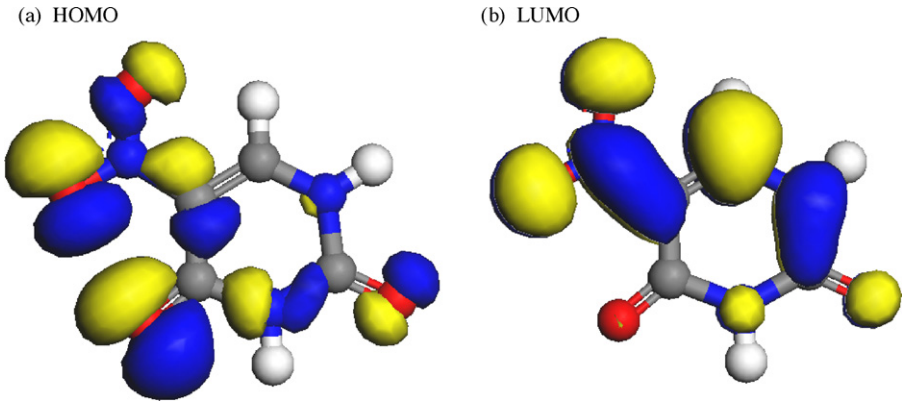

Fig. 3. The geometry and the highest occupied and the lowest unoccupied molecular orbitals (HOMO and LUMO, respectively) of 5-nitrourcil optimized in DMol3.

electrons with energies close to zero eV. The peak at 157 Da corresponds to parent ions, at higher masses the isotopes of $5NU^-$ are also detected. The isotopic distribution presented in Fig. 2 agrees with calculated one. The formation of parent ions was also observed in other 5-substituted (halogenated) uracil derivatives, e.g., 5-chlorouracil [18–20,24,25], 5-bromouracil [17,18,20–23]. Close to 0 eV, electron attachment to 5NU may lead to the creation of either a "dipole-bound" or a "valence" anion. The former anionic species corresponds to the excess electron being weakly bound to the closed shell molecule via long-range forces and resides outside the molecular frame [32]. For a pure "dipole-anion", a minimum dipole moment of 2.0–2.5 D is required in order to form a stable molecular anion. The dipole moment of 5NU is calculated to be 6.2 D [33], and thus allowing a dipole-bound state to be formed. However, valence anions formed by location of an excess electron to one of the unoccupied orbitals is also possible. We have calculated the energies of HOMO, LUMO and LUMO + n, where n is an unoccupied orbital and equals to 1, 2, 3 and 4. The values for these orbitals are presented in Table 1. Fig. 3 shows representations of the wavefunctions for the HOMO and LUMO for 5NU. In this figure the positive lobes of the orbital are light blue and the negative lobes are yellow.

Additional information can be also obtained from a calculation of the distribution of charge over a surface of the molecule (electrostatic potential surfaces—EPS). Fig. 1b shows the geometry plus the electronic shape of the molecule. Low values of the potential (electron-rich regions) are coloured blue, while high values (electron-deficient regions) are coloured red. From the EPS map one can see that electrons will be attracted around hydrogen atoms, this is also in accordance with the shape of the LUMO.

The experimentally estimated life time of a $5NU^-$ parent anion is in the range of 250 μs which is comparatively long relative to either dissociation or electron autodetachment. Previous experimental studies on electron interactions with 5NU did not reveal the presence of a parent anion possibly due to the limited mass resolution which did not allow to separate $5NU^-$ and $(5NU–H)^-$ at zero energy [26]. However, above 0.05 eV, the $(5NU–H)^-$ anion is dominant and more easily separated.

Table 1
The values for HOMO, LUMO, and LUMO + n (where n = 1–4) of 5-nitrouracil calculated with DMol3

Molecular orbital	eV
HOMO	−6.4
LUMO	−3.6
LUMO + 1	−2.5
LUMO + 2	−1.4
LUMO + 3	−0.1
LUMO + 4	+1.2

4.2. Dissociative electron attachment

The formation of negative ions is due to the dissociative electron attachment process, most likely via shape or core-excited resonances which are observed as a peak in the ion yield. At low energy (below 20 eV), electron interactions with the gas phase 5NU reveals a very rich fragmentation pattern, with 18 observed ions, shown in Figs. 4 and 5 and listed in Table 2.

The yields for the three most intense anions observed in the energy range of 0–2 eV, i.e., $(5NU–NO_2)^-$, $(5NU–H)^-$ and $(5NU–OH)^-$ were reported recently [26]. These anions are characterized by large cross-sections ($\geq 10^{-14}$ cm^2) clearly showing resonant features close to zero energy. However, in the present study these two peaks overlap due to the poor energy resolution of the VG-ZAB. Almost all heavy anions (presented in Fig. 4) with mass above 96 Da show resonant structures below 3 eV.

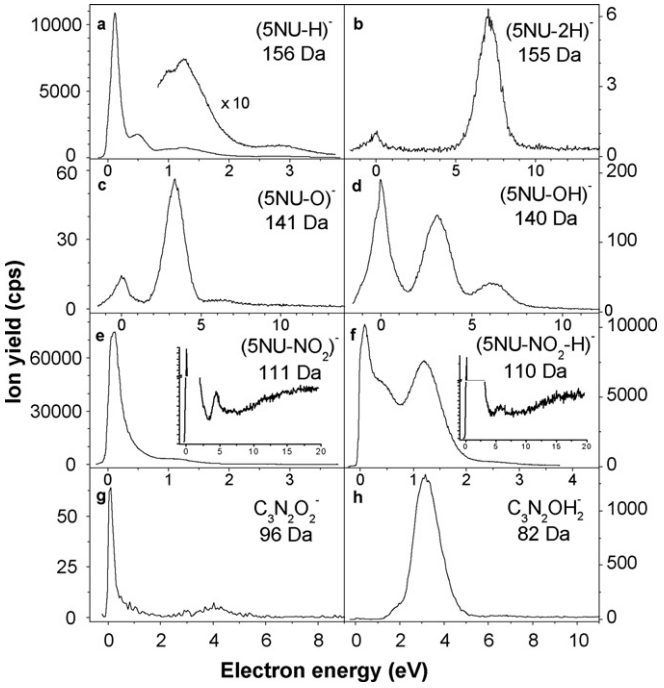

Fig. 4. Anion yields as a function of the incident electron energy for heavier mass fragments (above 82 Da) formed via DEA to 5-nitrouracil.

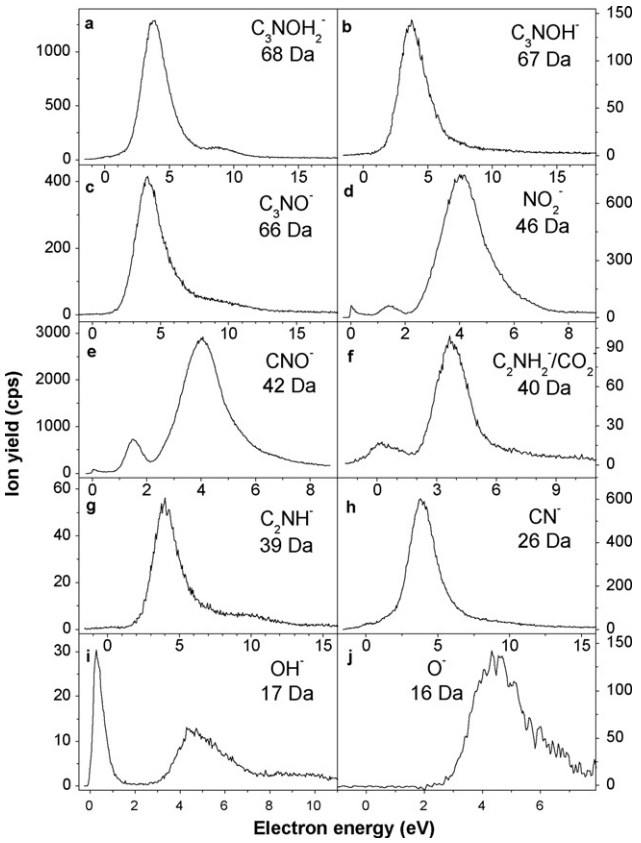

Fig. 5. Anion yields of the incident electron energy for the 10 lighter mass fragments formed via DEA to 5-nitrouracil.

In contrast to uracil [31] and other nucleobases [27,34,35] the dehydrogenated molecular fragment $(5NU–H)^-$ is not the most dominant fragment produced via DEA. H loss from nucleobases is observed explicitly from nitrogen atoms in purine and pyrimidine rings [36,37]. Energy thresholds of 0.12, 0.83 and 1.66 eV obtained from previously calculated dissociation energies and electron affinities for particular bonds in 5NU, i.e., N(1)–H, N(3) and C(6)–H, respectively, show that all dissociation channels are energetically favourable [26]. However, it is worth noting that there is an antibonding interaction in the C(6)–H bond in the LUMO, shown in Fig. 3b.

The ion yield for $(5NU–2H)^-$, presented in Fig. 4b, is formed due to the loss of two hydrogen atoms and it resembles those observed for uracil [31]. The formation of this ion involves electrons with energies close to zero eV, but the main peak in the energy spectrum is located at 7 eV. Moreover, experiments with deuterated thymine and calculations have shown that the low energy signal is due to removal of an intact hydrogen molecule, in that case the binding energy of H_2 reduces the required energy by 4.54 eV, whereas a higher energy signal is due to a loss of two independent hydrogen atoms [38].

The formation of the $(5NU–O)^-$ anion (Fig. 4c) was not observed in the case of uracil [31], therefore it can be attributed to loss of an oxygen atom from the nitro group. This ion yield shows two peaks with maxima located around 0 and 3 eV and a weak diffuse structure at 6 eV, similar to that for $(5NU–OH)^-$ but with different relative intensities (Fig. 4d). The energy threshold for the production of $(5NU–OH)^-$ from 5-nitrouracil and its isomer (enol form) was computed at 1.82 and 0.66 eV, respectively [26]. Moreover, the second peak observed at around 3 eV corresponds to the value of a gap between HOMO and LUMO (Table 1), i.e., 2.8 eV. Thus the formation of this ion by 3 eV electrons can be attributed to the capture of an excess electron to the lowest virtual molecular orbital. However the existence of the 6 eV peak can be explained by either the attachment to one of the higher unoccupied molecular orbitals or the formation of Feshbach core excited resonances (i.e., formation of a two-electron-one-hole molecular anion).

The most abundant signal is observed for the $(5NU–NO_2)^-$ anion (Fig. 4e), the complementary ion, i.e., NO_2^- is also detected but at higher energies and with two orders of magnitude less signal (see Fig. 5d). Taking the value of the dissociation energy of the C–NO_2 bond (3.13 eV) [26] in 5NU and the well-known electron affinities of the NO_2 group (2.27 eV) and the $(5NU–NO_2)$ radical (2.26 eV) [26] an energy threshold of 0.8 eV is estimated, however the observed threshold from experiment is much lower. Fig. 3b shows that the LUMO is localized around C–NO_2 indicating the strong electron bonding interaction, moreover the nitro group may also interact with electrons of the uracil ring leading to intermolecular charge transfers and to formation of different mesomeric form of this molecule [33]. Moreover, the $(5NU–NO_2)^-$ anion can be formed via metastable decay of the parent molecular anion. The MIKE scan of $5NU^-$ formed upon zero eV electron attachment losing the NO_2 group is presented in Fig. 6. From the intensity ratio of both peaks,

Table 2
Mass, empirical formula of the ions and the peak positions for all observed ions formed upon DEA to 5-nitrouracil

Mass (Da)	Molecular formula of an anion	Resonance positions (eV) ±0.10 eV
157	$C_4N_3O_4H_3^-$	0.00
156	$C_4N_3O_4H_2^-$	0.12, 0.49, 1.00, 1.27, 2.90
155	$C_4N_3O_4H^-$	0.00, 7.05
141	$C_4N_3O_3H_3^-$	0.00, 3.35, 6.35
140	$C_4N_3O_3H_2^-$	0.10, 3.05, 6.30
111	$C_4N_2O_2H_3^-$	0.07, 1.05, 4.40
110	$C_4N_2O_2H_2^-$	0.12, 0.50, 1.25, 5.80
96	$C_3N_2O_2^-$	0.10, 4.03
82	$C_3N_2OH_2^-$	2.00, 3.20
68	$C_3NOH_2^-$	3.70, 8.95
67	C_3NOH^-	3.70
66	C_3NO^-	3.95, 9.00
46	NO_2^-	0.01, 1.36, 4.00
42	CNO^-	0.06, 1.50, 3.99
40	C_2NH_2/CO_2^-	0.05, 3.65
39	C_2NH^-	4.00, 9.80
26	CN^-	3.85
17	OH^-	0.27, 4.56
16	O^-	4.27

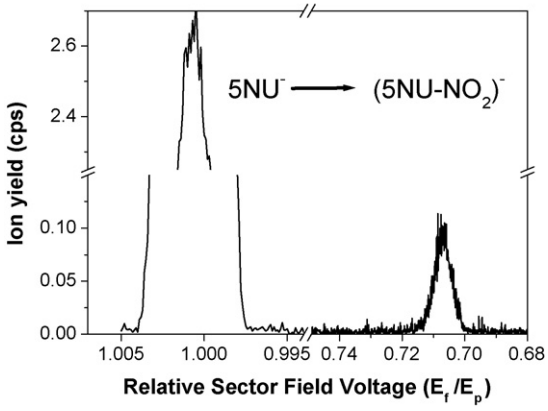

Fig. 6. MIKE spectrum showing the loss of NO_2 via metastable decay of $(5NU)^-$ through DEA. Stable parent ions of mass m_p pass the electrostatic sector at the voltage E_p; fragment ions m_f produced between the magnetic and the electrostatic sectors pass at the reduced voltage $E_f = E_p m_f/m_p$.

4% of the total amount of parent anions decay to $(5NU–NO_2)^-$ in our experimental time window.

The ion yield observed for the mass 110 Da (Fig. 4f) corresponding to simultaneous loss of the nitro group and one hydrogen atom shows many resonant features at energies listed in Table 2.

The formation of anions with mass 96 Da can be attributed to $C_3N_2O_2^-$, the ion signal being relatively weak; however, it shows a sharp structure at zero eV. The production of this ion cannot to be explained by the rupture of any particular bond, therefore molecular rearrangement due to electron attachment to 5NU has to be involved.

All negative ions detected at masses below 82 Da (shown in Figs. 4h and 5a–j) are produced in the energy range between 3 and 6 eV. The formation of resonances at these energies is possible if an excess electron occupies one of the virtual molecular orbitals; the energy levels computed for such unoccupied MO's are listed in Table 1. The values of HOMO and unoccupied orbital (LUMO and LUMO + n, where $n = 1–4$) gaps are 2.804, 3.977, 5.086, 6.331 and 7.601 eV. Another possibility for the origin of these negatively charged fragments is production via Feshbach core excited resonances, where an excess electron excites one of the bound electrons and is simultaneously captured by the molecule. A recent study on electronic excitation of 5NU reported three bands in the electron energy range of 3–6 eV, namely at 3.7, 4.76 and 5.72 eV [26].

In addition to the 3–6 eV structure, yields of NO_2^- and CNO^- show a weak feature with the maximum at 1.5 eV, in Fig. 5d and e, respectively. Moreover, the OH^- ion, which is considered to originate as a complementary reaction channel to the formation of the $(5NU–OH)^-$ anion also exhibits a zero eV peak in the energy spectrum (Fig. 5i), however with an intensity one order of magnitude lower than those in Fig. 4d.

It is worth noting that ions with masses 68, 67, 66, 42, 40 and 26 Da were also detected for uracil [31]. However the resonances observed for these masses in 5NU are located at significantly lower energies. This shift towards lower energies shows the strong influence of the nitro group on the electron attachment process leading to the formation of these fragments. However in contrast, the yield of the O^- anion below 8 eV (Fig. 5j) resembles that from uracil, in both the shape and the location of maximum of a peak, i.e., about 4 eV. Therefore the formation of this ion can be attributed to the oxygen loss from the C=O bond in the pyrimidine ring.

5. Conclusions

Experimental studies performed on low energy (below 20 eV) electron impact on gas phase 5-nitrouracil show the formation of a long-lived parent anion, as well as a rich fragmentation pattern. Fragmentation is attributed to DEA via resonant capture of the incident electron into either shape or core excited resonances. A comparison of present results with those for uracil indicates that dissociation of gas phase 5NU is more efficient and involves electrons with lower energies. These properties of 5-nitrouracil show its radiosensitizing nature, which is likely to be similar to that of the halogenated uracils.

The observed electron attachment process leads to complex molecular decomposition over the studied energy range and induces the formation of many different anions and radical fragments. If they are formed within DNA, some of these fragments may react and thus lead to activation of lethal cluster damage in living cells.

Acknowledgments

This work was financially supported by Engineering and Physical Sciences Research Council EPSRC (EP/D067138/1). This work was also supported by the FWF, Wien, Austria and the EU Commission, Brussels.

References

[1] H.L. Howe, P.A. Wingo, M.J. Thun, L.A.G. Ries, H.M. Rosenberg, E.G. Feigal, B.K. Edwards, J. Nat. Cancer Inst. 93 (2001) 824.
[2] M. Saunders, S. Dische, A. Barrett, A. Havey, D. Gibson, M. Parmar, Lancet 350 (1997) 161.
[3] International Commission on Radiation Units and Measurements, ICRU Report 31 ICRU, Washington, DC, 1979.
[4] V. Cobut, Y. Frongillo, J.-P. Patau, T. Goulet, J.-P. Jay-Gerin, Radiat. Phys. Chem. 51 (1998) 229.
[5] L. Sanche, Eur. Phys. J. D 35 (2005) 367.
[6] K.S. Jain, T.S. Chitre, P.B. Miniyar, M.K. Kathiaravan, V.S. Bendre, V.S. Veer, S.R. Shahane, C. Shishoo, J. Curr. Sci. 90 (2006) 793.
[7] D.B. Longley, D.P. Harkin, P.G. Johnston, Nat. Rev. 3 (2003) 330.
[8] D.J. Buschbaum, M.B. Khazaeli, M.A. Davis, Cancer 73 (Suppl.) (1994) 999.
[9] M. Chelladurai, C.A. Lobocki, M. Sultani, Y. Hanna, A. Drelichman, D.R. Pieper, P.W. McLaughlin, Cancer Chemother. Pharmacol. 40 (1997) 463.
[10] S. Zamenhof,. DeGiovanni, S. Greer, Nature 181 (1958) 827.
[11] W. Szybalski, Cancer Chemother. Rep. 58 (1974) 539.
[12] P. Wardman, E.D. Clarke, I.R. Flockhart, R.G. Wallace, Br. J. Cancer 37 (Suppl. III) (1978) 1.
[13] B.H. Lee, J.H. Shin, M.K. Lim, Bull. Korean Chem. Soc. 18 (1997) 734.
[14] P. Kranz, C.S. Lee, A.M. Gero, W.J. O'Sullivan, Biochem. Pharmacol. 38 (1989) 3785.
[15] A. Copik, J. Suwinski, K. Walczak, J. Bronikowska, Z. Czuba, W. Król, Nucleosides Nucleotides Nucleic Acids 21 (2002) 377.
[16] A. Gondela, K. Walczak, Tetrahedron Lett. 44 (2003) 7201;
A. Gondela, K. Walczak, Tetrahedron Lett. 4 (2006) 4653;
A. Gondela, K. Walczak, Tetrahedron 63 (2007) 2859.
[17] H. Abdoul-Carime, M.A. Huels, F. Brüning, E. Illenberger, L. Sanche, J. Chem. Phys. 113 (2000) 2517.
[18] H. Abdoul-Carime, M.A. Huels, E. Illenberger, L. Sanche, J. Am. Chem. Soc. 123 (2001) 5354.
[19] H. Abdoul-Carime, M.A. Huels, E. Illenberger, L. Sanche, Int. J. Mass Spec. 228 (2003) 703.
[20] S. Denifl, S. Matejcik, B. Gstir, G. Hanel, B.M. Probst, P. Scheier, T.D. Märk, J. Chem. Phys. 118 (2003) 4107.
[21] R. Abouaf, J. Pommier, H. Dunet, Int. J. Mass Spec. 226 (2003) 397.
[22] H. Abdoul-Carime, P. Limao-Vieira, S. Gohlke, I. Petrushko, N.J. Mason, E. Illenberger, Chem. Phys. Lett. 393 (2004) 442.
[23] S. Denifl, P. Candori, S. Ptasinska, P. Limao-Vieira, V. Grill, T.D. Märk, P. Scheier, Eur. J. Phys. D 35 (2005) 391.
[24] S. Denifl, S. Ptasińska, B. Gstir, P. Scheier, T.D. Märk, Int. J. Mass Spec. 232 (2004) 99.
[25] S. Denifl, S. Matejcik, S. Ptasińska, B. Gstir, M. Probst, P. Scheier, E. Illenberger, T.D. Märk, J. Chem. Phys. 120 (2004) 704.
[26] R. Abouaf, S. Ptasinska, D. Teillet-Billy, Chem. Phys. Lett. 455 (2008) 169.
[27] D. Huber, M. Beikircher, S. Denifl, F. Zappa, S. Matejcik, A. Bacher, V. Grill, T.D. Märk, P. Scheier, J. Chem. Phys. 125 (2006) 084304, and references therein.
[28] R.G. Cooks, J.H. Beynon, R.M. Caprioli, G.R. Lester, Metastable Ions, Elsevier, Amsterdam, 1973.
[29] S.C. Chu, P.D. Burrow, Chem. Phys. Lett. 172 (1990) 17.
[30] Materials Studio DMol3 version 4.2 (2007).
[31] S. Denifl, S. Ptasinska, G. Hanel, B. Gstir, M. Probst, P. Scheier, T.D. Märk, J. Chem. Phys. 120 (14) (2004) 6557.
[32] D.C. Clary, J. Phys. Chem. 92 (1988) 3173.
[33] G. Puccetti, A. Perigaud, j. Badan, I. Ledoux, J. Zyss, J. Opt. Soc. Am. B 10 (1993) 733.
[34] S. Denifl, S. Ptasinska, M. Cingel, S. Matejcik, P. Scheier, T.D. Märk, Chem. Phys. Lett. 377 (2003) 74.
[35] S. Denifl, S. Ptasińska, M. Probst, J. Hrusak, P. Scheier, T.D. Märk, J. Phys. Chem. A 108 (31) (2004) 6562.
[36] S. Ptasińska, S. Denifl, P. Scheier, T.D. Märk, E. Illenberger, Angew. Chem. Int. Ed. 44 (2005) 6941.
[37] H. Abdoul-Carime, s. Gohlke, E. Illenberger, Phys. Rev. Lett. 92 (2004) 168103.
[38] S. Ptasińska, S. Denifl, B. Mróz, M. Probst, V. Grill, E. Illenberger, P. Scheier, T.D. Maerk, J. Chem. Phys. 123 (2005) 124302.